Available online at www.sciencedirect.com

ScienceDirect

Energy Procedia 101 (2016) 854 – 861

Energy Procedia

71st Conference of the Italian Thermal Machines Engineering Association, ATI2016, 14-16 September 2016, Turin, Italy

Renewable energy storage system based on a Power-to-Gas conversion process

M. A. Ancona[a,]*, G. Antonioni[a], L. Branchini[a], A. De Pascale[a], F. Melino[a], V. Orlandini[a]

V. Antonucci[b], M. Ferraro[b]

[a]*Alma Mater Studiorum - Università di Bologna, Viale del Risorgimento 2, Bologna 40136, Italy*
[b]*CNR-ITAE, Salita S. Lucia sopra Contesse 5, Messina 98126, Italy*

Abstract

The increasing penetration of renewable energy generation in the electric energy market is currently posing new critical issues, related to the generation prediction and scheduling, due to the mismatch between power production and utilization. In order to cope with these issues, the implementation of new large scale storage units on the electric network is foreseen as a key mitigation strategy.
Among large scale technologies for the electric energy storage, the Power-to-Gas solution can be regarded as a long-term viable option, provided that the conversion efficiency is improved and aligned with other more conventional storage alternatives.
In this study, a Power-to-Gas storage system is investigated, including as main components a high-temperature electrolyzer for hydrogen generation and a Sabatier reactor for methane production. The high-temperature Solide Oxide Electrolyser Cell (SOEC) technology, currently under development, is considered as a promising solution for hydrogen generation, due to the expected higher efficiency values, in comparison with conventional low-temperature electrolysis technologies. In order to evaluate the performance of the system and the energy efficiency, in this study a numerical model of the SOEC integrated with the Sabatier reactor has been implemented, including also the necessary additional auxiliaries, which can significantly affect the energy conversion performance. The whole energy conversion and storage system has been analyzed, taking into account different layout variants, by means of Aspen Hysys™ numerical tool, based on a lumped modelling approach.
The various Power-to-Gas storage configurations have been compared, with the aim to optimize both the system's efficiency and the composition of the produced gas stream.

* Corresponding author. Tel.: +39-051-2093320; fax: +39-051-2093313.
E-mail address: maria.ancona2@unibo.it

doi:10.1016/j.egypro.2016.11.108

Keywords: Power-to-Gas; syngas; optimization; storage systems

1. Introduction

Significant technology developments and cost reduction occurred in the renewable energy sector [1], making wind and solar energy more competitive in comparison with many conventional power generation plants. As a consequence, the energy market is facing increasing penetration rates of renewables in the last few years. Renewable sources contributed nearly half of the world's new power generation capacity in 2014 and the trend is expected to grow [2]. The increasing non-programmable renewable shares in generated power is causing additional challenges for the existing electric energy distribution networks [3-5], due to the stochastic nature of wind and solar power production. When intermittent renewables are integrated into the network, issues arise in terms of power quality, voltage stability, reliability, etc. [6], requiring additional flexibility margins for the electricity system. In order to accommodate increasing rates of non-programmable renewable electric power into the existing electric network, grid-scale energy storage is believed to be a solution [7] able to add the required flexibility to the power system. Among the key requisites for a competitive energy storage system, Castillo & Gayme [7] identified: capacity, energy and power density, typical power size, roundtrip efficiency, charge/discharge duration, response time, lifetime and cost. The state-of-the-art of the various electric energy storage technologies has been reviewed in many recent studies, see for example [6-10]; these studies highlight Pumped Hydro Storage (PHS) and Compressed Air Energy Storage (CAES) as the two solutions available for largest capacities (up to 8000 MWh for PHS and around 2000 MWh for CAES), largest power size (up to 5000 MW for PHS and 300 MW for CAES) and with lowest specific costs (10÷100 €/kWh and 3÷70€/kWh, respectively), in comparison with all different batteries [6, 10]. Nevertheless, PHS and CAES are still limited in capacity and other strategies could become more competitive for very large scale energy storage. In particular, electricity could be used to produce synthetic gaseous fuels, in the framework of a Power-to-Gas concept, as illustrated in [11]. The possibility to exploit the existing natural gas distribution network allows to conceive theoretically infinite storage capacity, but efficiency issues of the process should be deeply analyzed.

In this context, the P2G system allows to obtain synthetic natural gas (syngas) starting from the electric energy produced from non-programmable renewable energy sources (*i.e.* photovoltaic and wind technologies). A schematic of the whole process – from the electric energy to the final user – is presented in Figure 1, including also the Natural Gas (NG) network and the reconversion system to obtain electricity and/or heat.

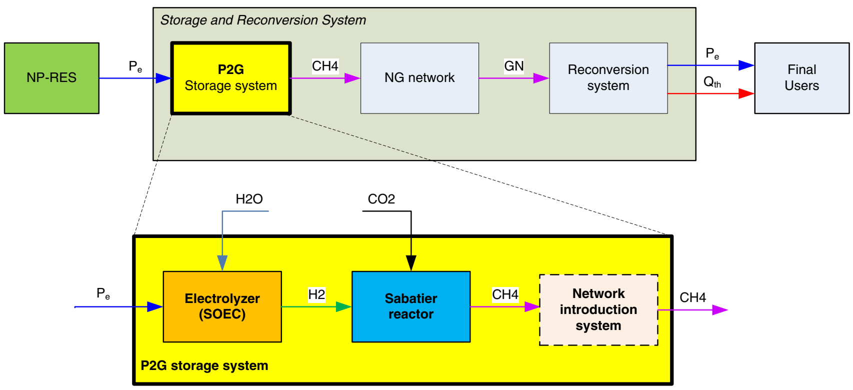

Fig. 1. Power-to-Gas storage system.

This study focuses only on the proper P2G storage system (in yellow in Figure 1), composed of three main components:

- the electrolyzer, for the production of hydrogen starting from electric power and water according to the following reaction:

$$H_2O \rightarrow H_2 + \frac{1}{2}O_2$$

Since the conversion rate increases with the temperature, in this study high temperature electrolysis has been considered by accounting the innovative Solid Oxide Electrolysis Cell (SOEC), generally operating in the temperature range of 600÷1000°C. This technology allows to obtain very high efficiency (around the 90%) thanks to the high temperature operation and it is characterized by the solid state of components, avoiding corrosion and electrolyte evaporation problems [12-14].

- the Sabatier reactor, for the production of synthetic natural gas starting from hydrogen and CO_2 by means of the following reaction [11, 15, 16]:

$$CO_2 + 4H_2 \rightarrow CH_4 + 2H_2O$$

This reaction requires metal catalysts to occur and the optimum process temperature ranges from 250 to 400 °C [17].

- the system for the gas introduction into the network, mainly consisting of compression stages.

2. Calculation model and assumptions

In this study, various configurations of P2G storage system have been modeled and simulated in Aspen Hysys^{TM} environment [18], in order to determine an optimum solution in terms of both energy conversion efficiency and percentage of produced CH_4 (*i.e.* conversion yield). In more detail, the analysis has been started with a Reference Case (see Figure 2 *(a)*), where three main steps can be identified: *(i)* SOEC electrolyzer, *(ii)* Sabatier reactor and *(iii)* compression train. In this configuration the water feed of the SOEC is heated by means of an external heat source, to reach the adequate temperature level for the electrolysis reaction. After the reaction, the oxygen is separated from the hydrogen stream thanks to a sweep air stream; both the hydrogen and the oxygen are then cooled to the ambient temperature (25 °C). In particular, the need of cooling the hydrogen stream before entering the Sabatier reactor is due to the presence of water, which can be thus eliminated (separator SEP 1 in Figure 2 *(a)*) after condensation. For the same reason, also the methane stream at the outlet of the Sabatier reactor is cooled and the condensed water separated (SEP2 in Figure 2 *(a)*). Finally, the methane stream is compressed by means of an inter and after-cooled compression train, in order to reach the network pressure and contemporarily minimize the electric energy consumption. The main input data of the simulation for the Reference Case are listed in Table 1. The values of the involved parameters have been chosen on the basis of available literature in order to operate each component in optimum conditions.

Starting from the above-described layout, three modifications have been considered, named respectively Case 1 (see Figure 2 *(b)*), Case 2 (see Figure 2 *(c)*) and Case 3 (see Figure 2 *(d)*). Differently to the Reference Case, all these plant configurations consider heat recovery from suitable process' sections, in order to pre-heat the inlet feed water stream of the SOEC. In more detail, Case 1 differs from Reference Case only concerning the recovery of the heat hailing – in order of succession – from the sweep air cooling, the Sabatier outlet stream and the SOEC outlet stream. The choice of the heat to be recovered and the order of the recovery itself have been established considering the temperature levels of the available heat. Relating to Case 2 and Case 3, instead, the heat recovery is equivalent to Case 1, but a further layout modification is considered with respect to the Reference Case: in Case 2, indeed, the compression section has been moved before the Sabatier reactor, while in Case 3 the compression section has been split into two parts, respectively before and after the Sabatier reactor. The specific assumptions made for the simulations of these three layouts are presented in Table 2. All the remaining parameters have not been modified with respect to the Reference Case.

Table 1. Reference Case main operating parameters.

Parameter	Value	Units
Inlet H_2O temperature	25	°C
SOEC input electric power	1	MW
SOEC operating temperature	850	°C
SOEC operating pressure	1	bar
SOEC conversion effectiveness	80	%
Sweep air temperature	25	°C
Sweep air pressure	1	bar
$O_{2,\ sweep}/O_{2,\ produced}$ ratio	2	-
Outlet SEP 1 saturation	100	%
Sabatier operating temperature	350	°C
Sabatier operating pressure	1	bar
CO_2/H_2 molar inlet fraction	1/4	-
$CO/(CO_2+CO)$ molar inlet fraction	20	%
Inlet Sabatier reactants temperature	25	°C
Inlet Sabatier reactants pressure	1	bar
C1 and C2 coolers outlet temperature	25	°C
Compressed syngas pressure	60	bar
COMP1 and COMP2 compression ratio	7.75	-
COMP1 and COMP2 isentropic efficiency	80	%
Inter and after-cooling temperature	25	°C

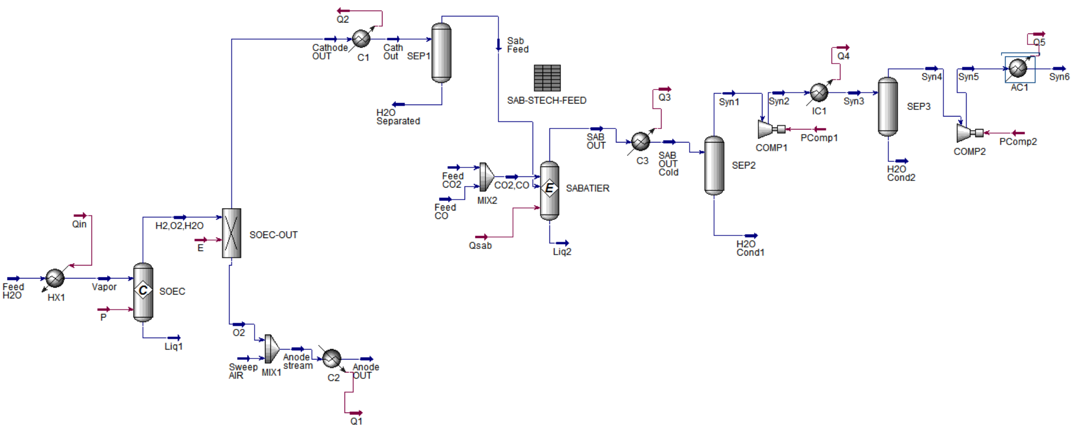

(a)

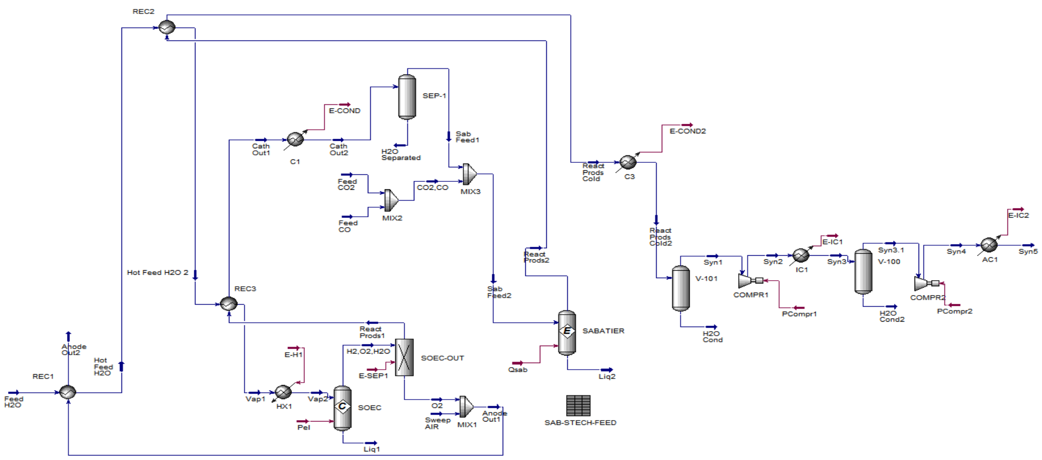

(b)

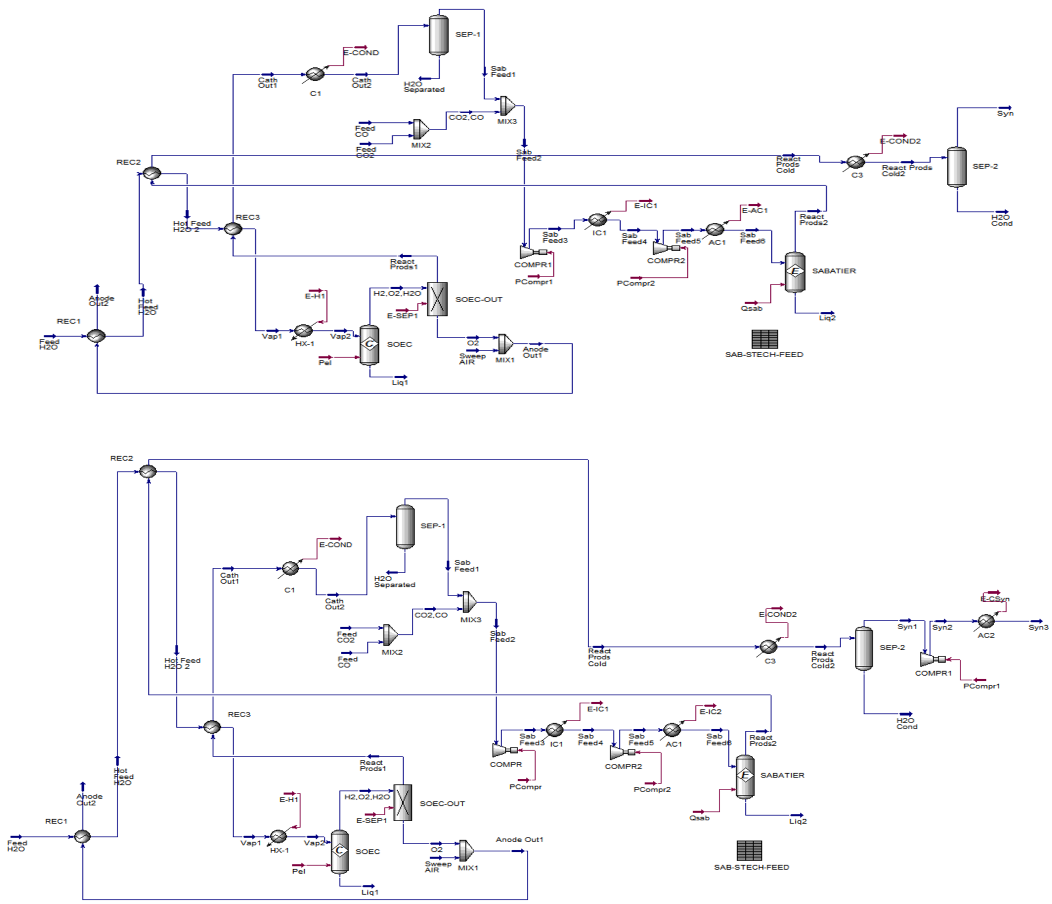

(c)

(d)

Fig. 2. Case studies' layouts: *(a)* Reference Case – no thermal recover, *(b)* Case 1, *(c)* Case 2 and *(d)* Case 3.

Table 2. Specific input data for Case 1, Case 2 and Case 3.

Parameter	Case 1	Case 2	Case 3
REC1, REC2 and REC 3 minimum temperature difference between outlet hot side and inlet cold side	5 °C	5 °C	5 °C
Inlet Sabatier reactants temperature	25 °C	25 °C	25 °C
Inlet Sabatier reactants pressure	1 bar	60 bar	30 bar
COMP1 compression ratio	7.75	7.75	5.48
COMP2 compression ratio	7.75	7.75	5.48
COMP3 compression ratio	-	-	2
Compressors isentropic efficiency	80%	80%	80%

In order to evaluate and compare the performance of the presented P2G system configurations, two efficiency indices have been considered in this study. The first index is the electric-to-fuel conversion efficiency, defined as follows:

$$\eta_{E2F,P2G} = \frac{m_{SYN} \cdot LHV_{SYN}}{P_{e,NP-RES} + P_{e,COMP}} \tag{1}$$

where both the electric power required for the compression and the electric power from non-programmable renewable energy sources to produce hydrogen are considered.

However, this index doesn't account for the thermal energy exchange due to the eventual heat recovery. For this reason, the electric-to-fuel efficiency is not thorough to describe and evaluate the performance of the P2G storage system. As a consequence, in the carried-out analysis also the first law efficiency of the whole P2G system has been estimated:

$$\eta_{I,P2G} = \frac{m_{SYN} \cdot LHV_{SYN}}{P_{e,NP-RES} + P_{e,COMP} + \sum Q_{th,IN} - \sum Q_{th,R}} \quad (2)$$

where $\sum Q_{th,IN}$ represents the total required heat and $\sum Q_{th,R}$ the sum of the recovered heat (eventually present) from sections of the process where heat removal is necessary.
Furthermore, with the purpose of estimating which is the less performant component, the evaluation of the first law efficiency can be extended also to the various components of the system, *i.e.* to the main sections of the process (SOEC and Sabatier), obtaining the following expressions:

$$\eta_{I,SOEC} = \frac{m_{H_2} \cdot LHV_{H_2}}{P_{e,NP-RES} + \sum_{SOEC} Q_{th,IN} - \sum_{SOEC} Q_{th,R}} \quad (3)$$

$$\eta_{I,Sabatier} = \frac{m_{SYN} \cdot LHV_{SYN}}{m_{H_2} \cdot LHV_{H_2}} \quad (4)$$

Finally, the comparison analysis has been completed with the evaluation of the following parameters:

- composition of the produced synthetic natural gas stream: this parameter is fundamental in order to respect the framework for the gas introduction into the networks (*i.e.* a maximum percentage of hydrogen is authorized);
- Lower Heating Value (LHV) of the produced synthetic natural gas stream;
- Wobbe index of the produced synthetic natural gas stream, which is an indicator of the interchangeability of fuel gases with respect to natural gas, usually used to compare the combustion energy output of different composition fuels.

3. Results and discussion

The main results of the carried-out analysis are shown in Figures from 3 to 6. In more detail, for the case studies, in Figure 3 the histogram of the electric-to-fuel and of the first law efficiencies of the whole P2G system is presented, while in Figure 4 the first law efficiency values of SOEC and Sabatier reactor are plotted. From Figure 3 it can be noted that the electric-to-fuel efficiency results higher (equal to the 85%) for the Reference Case and Case 1, due to the higher compression work needed in Cases 2 and 3 (being equal the total compression ratio for all the considered cases, the position of the compression train obviously affect the efficiency results, *i.e.* the mass flow rate to be compressed changes). On the other hand, the first law efficiency acquires its maximum value in Cases 1 and 3 (around 72%), due to the heat recovery not considered for the Reference Case. In any case, the value of first law efficiency is always higher for the modified configurations with respect to the Reference Case. Moreover, if considering separately the contribution of the SOEC and of the Sabatier reactor (see Figure 4), it can be seen an opposite behavior for the two components: while first law efficiency for SOEC is maximum in cases 2 and 3 (equal to about the 89%), this parameter for the Sabatier reactor presents the higher value for Case 1 (89%) but for cases 2 and 3 it is lower than for the Reference Case. This evidence is due to the different plant configuration and it seems to indicate Case 1 as the best performing solution.

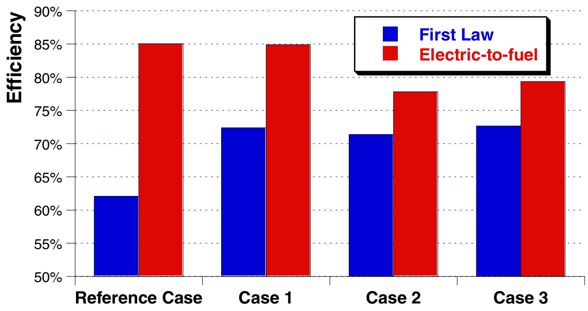

Fig. 3. Electric-to-fuel and first law efficiencies for the analyzed cases.

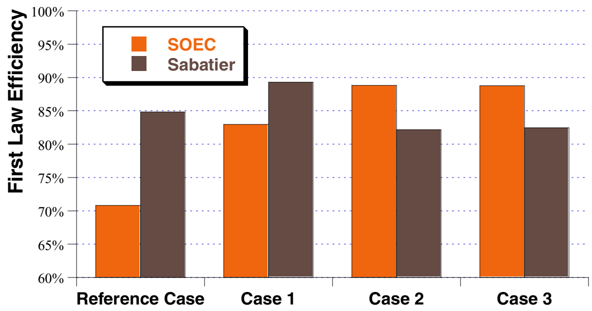

Fig. 4. First law efficiency values for SOEC and Sabatier separately.

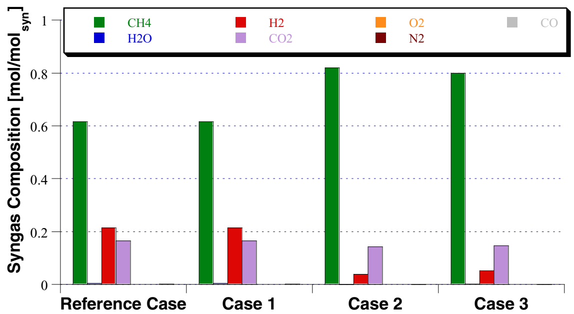

Fig. 5. Syngas composition at the end of the process.

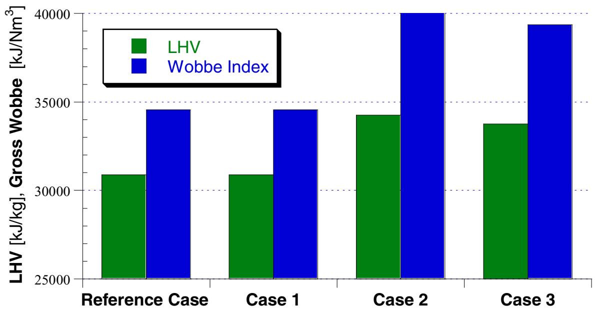

Fig. 6. Syngas LHV and Wobbe index at the end of the process.

However, as previously explained, the composition of the produced syngas is essential to allow the introduction of the fuel into the network. The molar fractions of the various chemical elements composing the produced syngas stream are shown in Figure 5 for the four analyzed cases. From the figure it can be observed that, even if Case 1 enables to achieve the best performance in terms of efficiency, the percentage of hydrogen content within the syngas stream is very high (equal to more than the 20%), avoiding the possibility to insert the fuel into the network. On the other hand, cases 2 and 3 allow to obtain a syngas stream with a high methane content (being maximum and equal to the 82% for Case 2) and contemporarily with low content of hydrogen (equal or less to the 5%) and CO_2. Water and CO are present only as trace elements, while oxygen and nitrogen are completely absent.

Finally, in Figure 6 the LHV and the Wobbe index of the produced syngas stream are shown. The obtained values for these quantities, together with the composition and the efficiencies results, suggest Case 2 (LHV=34000 kJ/kg and Wobbe index equal to 40000 kJ/Nm^3) as the best configuration for the P2G system.

4. Concluding remarks

Within a context where the penetration in the electric energy market of renewable energy sources is continuously increasing, storage systems become essential, in order to avoid problems linked to the mismatch between power production and users need. Among large scale technologies for the electric energy storage, the Power-to-Gas solution can be seen as an interesting viable option, allowing to obtain synthetic natural gas from non-programmable energy sources and CO_2 sequestration.

In this study, a new configuration – with high temperature electrolyzer (SOEC) – for the P2G storage system has been proposed (Reference Case). Furthermore, three different solutions have been developed and analyzed in order to optimize the system performance by the heat recovery and by evaluating the optimum position of the compression stages. The various P2G storage configurations have been compared considering both the electric-to-fuel and the first law efficiency; moreover, the synthetic natural gas composition, the LHV and the Wobbe index have been evaluated.

The results show that the heat recovery, to pre-heat the water at the inlet of the electrolyzer, allows to obtain always a performance increase (being maximum for Case 1). On the other hand, the position of the compression section considerably affects the percentage of CH_4 within the produced syngas stream and – as a consequence – also the corresponding LHV and Wobbe index. If considering these parameters, and contemporarily not penalizing the process efficiency too much, the analysis seems to indicate Case 2 as the optimum solution.

Nomenclature

C	Cooling heat exchanger
CAES	Compressed Air Energy Storage
COMP	Compressor
e	Electric
E2F	Electric-to-Fuel
IN	Inlet
LHV	Lower Heating Value
m	Mass flow rate
NG	Natural Gas
NP-RES	Non-Programmable Renewable Energy Sources
P	Power
PHS	Pumped Hydro Storage
P2G	Power-to-Gas
Q	Heat
R	Recovered
REC	Recuperator
SEP	Separator
SOEC	Solid Oxide Electrolyzer Cell
SYN	Syngas
th	thermal

References

[1] Renewable power generation costs in 2014, IRENA, 2015.
[2] World Energy Outlook 2015, IEA, 2015.
[3] Singh M, Khadkikar V, Chandra A, Varma RK. Grid interconnection of renewable energy sources at the distribution level with power-quality improvement features. IEEE Trans. 2011;26:307-315.
[4] Denholm P, Hand M. Grid flexibility and storage required to achieve very high penetration of variable renewable electricity. Energy Policy 2011;39:1817-1830.
[5] Jiang R, Wang J, Guan Y. Robust unit commitment with wind power and pumped storage hydro. IEEE Trans. 2012;27:800-810.
[6] Akinyele DO, Rayudu RK. Review of energy storage technologies for sustainable power networks. Sust Energ Tech and Ass 2014;8:74-91.
[7] Castillo A, Gayme DF. Grid-scale energy storage applications in renewable energy integration: a survey. Energ Convers Manage 2014;87:885-894.
[8] Luo X, Wang J, Dooner M, Clarke J. Overview of current development in electrical energy storage technologies and the application potential in power system operation. Applied Energy 2015;137:511–536.
[9] Beaudin M, Zareipour H, Schellenberglabe A, Rosehart W. Energy storage for mitigating the variability of renewable electricity sources: An updated review. Energy for Sustainable Development 2010;14:302-314.
[10] Díaz-González F, Sumper A, Gomis-Bellmunt O, Villafáfila-Robles R. A review of energy storage technologies for wind power applications. Renew Sust Energ Rev 2012;16:2154-2171.
[11] Schiebahn S, Grube T, Robinius M, Tietze V, Kumar B, Stolten D. Power to gas: Technological overview, systems analysis and economic assessment for a case study in Germany. Int. J of Hydrogen energy 2015;40:4285-4294.
[12] Monnerie N., Roeb M., Houaijia A., Sattler C. Coupling of wind energy and biogas with a high temperature steam electrolyser for hydrogen and methane production. Green and sustainable chemistry 2014;4:60-69.
[13] H. Zhang, S. Su, X. Chen, G. Lin, J. Chen. Configuration design and performance optimum analysis of a solar-driven high temperature steam electrolysis system for hydrogen production. Int J Hydrogen Energy 2013;38:4298-4307.
[14] Ni M, Leung MKH, Leung DYC. An electrochemical model of a solid oxide steam electrolyzer for hydrogen production. Chem Eng Technol 2006;29:636-642.
[15] P. Sabatier and J.B. Senderens, C.R. Acad. Sci. Paris 1902;134:514.
[16] W.Wang, J. Gong. Methanation of carbon dioxide: an overview. Chem Sci Eng, 2011;5:2-10.
[17] K. P. Brooksa, J. Hua, H. Zhub, R. J. Kee. Methanation of carbon dioxide by hydrogen reduction using the Sabatier process in microchannel reactors. Chemical Engineering Science 2007;62:1161-1170.
[18] Aspen Hysys™; https://www.aspentech.com/